An Accurate Statistical Cell Delay Model Considering Multiple-Input Switching Effect

Jiajie Xu[1], Leilei Jin[2], Hao Yan[3]
School of Electronic Science & Engineering, Southeast University, Nanjing 210096, China
[123]The National ASIC System Engineering Technology Research Center
* Email:{jiajiex, jinleilei, yanhao}@seu.edu.cn

2023 International Symposium of Electronics Design Automation (ISEDA) | 979-8-3503-0451-0/23/$31.00 ©2023 IEEE | DOI: 10.1109/ISEDA59274.2023.10218568

***Abstract*—To restrict the storage overhead, traditional statistical static timing analysis (SSTA) employs a delay model that assumes only a single input switches for a cell during a transition, while all other side inputs are held constant. Nevertheless, ignoring the impact of multiple-input switching (MIS) can lead to an overestimation or an underestimation of a cell delay, causing over-designing for the timing margin. In this paper, we present a novel approach using expected scale factors to assess the impact of MIS on statistical timing analysis. Meanwhile, an accurate cell delay calibration method considering skewness and kurtosis is proposed to measure the +/-3σ cell delay. Tested by cells with TSMC 28nm technology, our model can estimate the +/-3σ point with similar accuracy comparing to state-of-the-art technology in single-input switching (SIS) mode. Moreover, in near-/sub-threshold voltage, the cell delay computed by our model in MIS mode differs from the SPICE-computed delay by less than 4%, which infers significant improvement over MIS delay models proposed by prior studies.**

***Index Terms*—Multiple input switching, statistical timing analysis, library characterization.**

I. Introduction

Statistical static timing analysis (SSTA) is suitable for timing signoff analysis in advanced technology. Industry explored several methods for handling process variation effects, such as Liberty Variation Format (LVF) [1]. Timing library generation for logic cells in these methods involves characterizing the output waveform and the delay between the input and output pins using an accurate circuit simulator. Similarly to industrial methods, state-of-the-art cell delay models such as log-skew-normal (LSN) [2] and log-extended-skew-normal (LESN) [3] characterizing the cell delay with SIS assumption, which assumes only a single input switches during a transition.

However, it has been shown that the MIS delay of a multiple-input cell can be much smaller (due to dip effect) or greater than the corresponding SIS delay [4]. Using the illustration of a 2-input NAND in Fig. 1, a falling input transition on pin A produce a rising transition on Pin Y. In the case of SIS, the voltage of pin B is held at VDD so only one PMOS device is activated (Fig. 1 (a)). Nevertheless, when falling signals arrive at Pin A and Pin B simultaneously or with little interval, a situation of MIS will happen (Fig. 1 (b)). Comparing to the case of SIS, the output load C_L is charged through two PMOS devices other than one concurrently in the MIS situation, which results in a reduction of the cell delay. Experiment results reveal that in an extreme MIS case (two input signals fall simultaneously), the cell delay can drop to roughly half of that estimated by the SIS model [5].

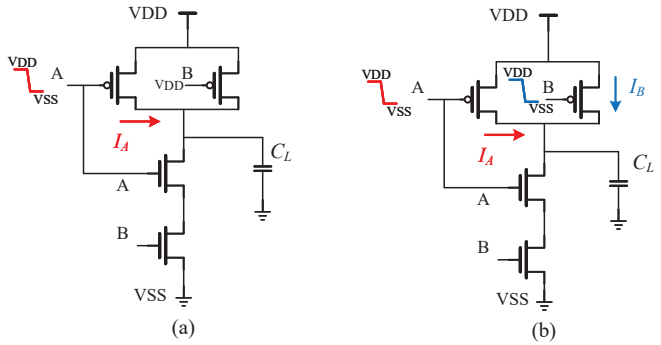

Fig. 1. (a) The single-input switching and (b) the multiple-input switching situations for a 2-input NAND cell.

Various models considering MIS effect have been adopted in statistical static timing analysis. Tang Q et. al propose a new transistor based stochastic cell delay model [6], while Sriharan J et al. construct the cell delay model through sampling [7]. Statistical projection and moment based delay calculation are also used in modelling statistical MIS effect [8]. A scale factor based deterministic timing analysis method is also extended to statistical area by Sinha D et al. and can be easily integrated to exiting statistical SIS model [9].

While prior work using various approaches to model MIS effect, the deterioration of cell delay distribution in near-/sub-threshold voltage is neglected. The cell delay distribution is considered to be a perfect Gaussian distribution in the previous statistical MIS models. However, as the voltage is scaled down, the process variation effect on the cell delay is not linear, which leads the distribution to have non-Gaussian features, represented as the asymmetry and the long tail [3]. As the tail shape and asymmetry of the delay distribution is not characterized, these models lead to large errors in estimating the +/-3σ delay of the delay distribution, causing over pessimism during designing.

In this paper, an accurate statistical cell delay model considering MIS effect is proposed. The main contributions can be summarized as follows:

1) A scale factor based MIS model is constructed to amend first and second moment of the cell delay. Closed form expressions for the scale factors is deduced and can be easily computed using existing software libraries.

2) The non-Gaussian features of the delay distribution are considered. The third and forth moment are used to capture

Authorized licensed use limited to: Chinese University of Hong Kong. Downloaded on November 22,2026 at 12:59:36 UTC from IEEE Xplore. Restrictions apply.

these features.

3) Experiments conducted with TSMC 28nm technology reveal our SIS mode delay model is competitive to state-of-the-art technology in near-/sub-threshold voltage, while MIS mode delay model shows an obvious promotion with former studies when estimating the +/-3σ delay.

II. Preliminary

Without any loss of generality, a scale factor based model can be used to depict the MIS-induced deterioration. Given the SIS delay d_i of an arc in a cell from input pin i to a certain output pin, the MIS delay d_{ij} of that arc with respect to a switching side input j is a function of the skew δ_{ij} between the arrival times of the input i and j, respectively. The scale factor in the MIS situation is denoted as $\Theta(\delta_{ij})$. Mathematically, it is defined as:

$$\Theta(\delta_{ij}) = \begin{cases} \theta + \frac{(1-\theta)|\delta|}{\eta} & |\delta| \le \eta \\ 1.0 & |\delta| > \eta \end{cases} \quad (1)$$

where, θ denotes the theoretical worst case scale factor for a given cell arc. The η denotes the bounds of the temporal proximity window within which MIS impacts cell delays, and is typically a function of the slew of the timing arc. $\Theta(\delta_{ij})$ is defined specifically for each cell type in the timing library that can be impacted by MIS. A similar model can also be applied to cell output-slews and increased cell delays resulted by MIS impact.

Nevertheless, in statistical timing analysis, the interval between the input i and input j is in the form of probability density function other than a constant number. As a result, the MIS delay d_{ij} in statistical analysis situation can not be simply calculated through (1). Further calculation is needed when applying the scale factor method in statistical timing analysis area.

III. Proposed Model

A. MIS model with cell delay calibration flow

The process of the cell delay calibration method with the MIS model proposed is given in Fig. 2. The scale factors and the relationship between moments and C_L are modelled through interpolation method based on SPICE MC simulations. Coefficients in the scale factors introduced in Section B is computed and saved. Moreover, the first four moments representing the statistical cell delay introduced in Section C are also stored. After that, given an input pair A and B, the statistical interval between them decides whether the MIS situation will occur. If the input signal pair truly affect each other, then the statistical scale factors are calculated and the first and second moment will be scaled. Finally, the delay calibration method proposed in Section C will be conducted.

B. Statistical MIS model based on scale factor

To ensure the timing yield during the chip signoff, the most important information for the designer are the 99.86% quantile as the worst-case delay and the 0.14% quantile as the best-case delay. In statistical timing analysis, the first two moments

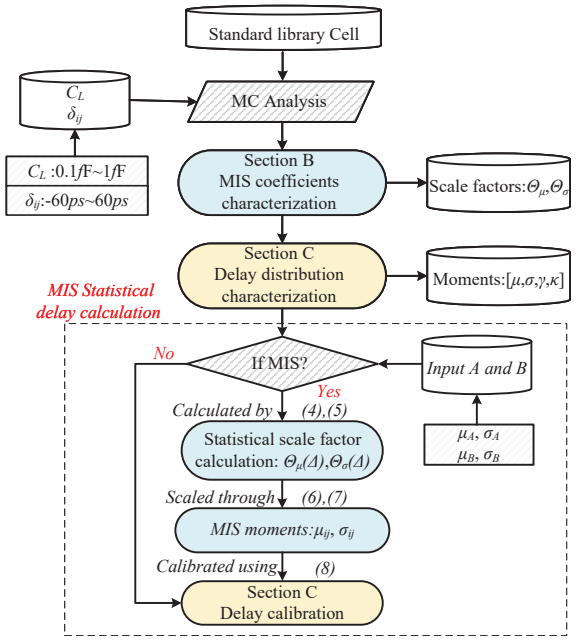

Fig. 2. The statistical cell delay calibration flow considering MIS effect.

(μ, σ) of a timing arc is needed to determine the worst-case and best-case arriving time, mathematically μ+3σ and μ-3σ, representing the 99.86% quantile and 0.14% quantile, respectively. So the relationship between the input arriving time skew and the first two moments of an NAND cell arc is constructed through 10k MC analysis, as shown in Fig. 3. The red lines represent the situation when the input signal of j arrives before the input signal of i ($\delta < 0$), while the blue lines stand for the opposite situation ($\delta > 0$). The first moment of the cell delay, mean (μ), can be reasonably captured by a similar linear scale factor shown in (1). Different from the first moment, the second moment of the cell delay, standard deviation (σ), needs a higher order regression. A quadratic scale factor is employed to capture the non-linearity of the standard deviation variation, mathematically:

$$\Theta(\delta_{ij}) = \begin{cases} \theta + \frac{(1-\theta)|\delta|}{\eta} + \xi(\delta^2 - \eta|\delta|) & |\delta| \le \eta \\ 1.0 & |\delta| > \eta \end{cases} \quad (2)$$

where, ξ represents to which extent the scale factor is deviated from a linear relationship. For convenience, the scale factor for the first moment of cell delay is denote as Θ_μ and for the second moment is denoted as Θ_σ in the rest of this paper.

However, in statistical timing analysis, the skew between two input signals is in the form of probability density function (PDF), other than a deterministic value. The statistical skew Δ_{ij} between the inputs is computed as a canonical form using statistical subtraction of the arrive times A_i and A_j. Assuming that A_i and A_j are mutually independent, and follow Gaussian distributions, then Δ_{ij} also follows a Gaussian distribution:

$$\Delta_{ij} \sim N(\mu_i - \mu_j, \sigma_i^2 + \sigma_j^2) \quad (3)$$

μ_i/μ_j represents the first moment for the distribution of A_i/A_j, while σ_i/σ_j represents the second moment. Under such

Authorized licensed use limited to: Chinese University of Hong Kong. Downloaded on November 22,2026 at 12:59:36 UTC from IEEE Xplore. Restrictions apply.

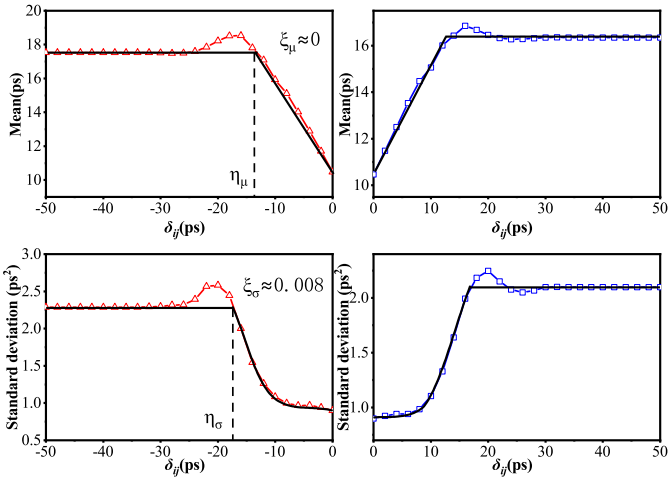

Fig. 3. First two moments variation of a 2-input NAND cell under deterministic skew (TSMC 28 nm, 0.6V) which can be captured by a quadratic scale factor given by (2).

assumption, a statistical scale factor can be deduced through calculating the mean value or expectation (E) of $\Theta(\Delta)$. The expected value of scale factor function of Θ_μ can be computed mathematically as:

$$\begin{aligned} E[\Theta_\mu(\Delta)] = &\int_{-\infty}^{\infty} \Theta_\mu(x)p(x)\mathrm{d}x \\ =&1.0 + (\theta-1)[\Phi(\frac{\eta-\mu}{\sigma}) - \Phi(\frac{-\eta-\mu}{\sigma})] \\ &+ \frac{(1-\theta)}{\eta}[2\phi(\frac{-\mu}{\sigma}) - 2\mu\Phi(\frac{-\mu}{\sigma})] \\ &- \frac{(1-\theta)}{\eta}[\phi(\frac{\eta-\mu}{\sigma}) + \phi(\frac{-\eta-\mu}{\sigma})] \\ &+ \frac{(1-\theta)}{\eta}[\mu\Phi(\frac{\eta-\mu}{\sigma}) + \mu\Phi(\frac{-\eta-\mu}{\sigma})] \end{aligned} \quad (4)$$

Similarly, the expected value of the scale factor function of Θ_σ can be computed mathematically as:

$$\begin{aligned} E[\Theta_\sigma(\Delta)] = &\int_{-\infty}^{\infty} \Theta_\sigma(x)p(x)\mathrm{d}x \\ =&1.0 + (\theta-1)[\Phi(\frac{\eta-\mu}{\sigma}) - \Phi(\frac{-\eta-\mu}{\sigma})] \\ &+ \frac{(1-\theta-\eta^2\xi)}{\eta}[2\phi(\frac{-\mu}{\sigma}) - 2\mu\Phi(\frac{-\mu}{\sigma})] \\ &- \frac{(1-\theta-\eta^2\xi)}{\eta}[\phi(\frac{\eta-\mu}{\sigma}) + \phi(\frac{-\eta-\mu}{\sigma})] \\ &+ \frac{(1-\theta-\eta^2\xi)}{\eta}[\mu\Phi(\frac{\eta-\mu}{\sigma}) + \mu\Phi(\frac{-\eta-\mu}{\sigma})] \\ &+ \sigma\xi[(-\eta+\mu)\phi(\frac{-\eta-\mu}{\sigma}) - (\eta+\mu)\phi(\frac{\eta-\mu}{\sigma})] \\ &+ \xi(\sigma^2+\mu^2)[\Phi(\frac{\eta-\mu}{\sigma}) - \Phi(\frac{-\eta-\mu}{\sigma})] \end{aligned} \quad (5)$$

where $\phi(x)$ represents the normal gauss distribution while Φ represents the Gaussian integral.

Thus, closed form expressions for the statistical scale factor functions of the first and second moment of a timing arc are obtained in (4) and (5) and can be easily computed. The first and second moment for MIS statistical delay of a timing arc can be easily obtained by:

$$\mu_{ij} = E[\mu_i * \Theta_\mu(\Delta)] = \mu_i * E[\Theta_\mu(\Delta)] \quad (6)$$

$$\sigma_{ij} = E[\sigma_i * \Theta_\sigma(\Delta)] = \sigma_i * E[\Theta_\sigma(\Delta)] \quad (7)$$

where μ_{ij} and σ_{ij} represent the first and second moment of statistical MIS delay. Then, the worst-case and best-case MIS delay can be calculated using $\mu_{ij} \pm 3\sigma_{ij}$. Comparing with Monte carlo based simulations, the accuracy losses of above equations are small.

C. Calibration of the +/-3σ point

As the voltage scaling down, the cell delay at the near-threshold regime becomes asymmetric and have a fatter tail. According to the theory proposed by Jin et. al in [3], these features can be captured by the third moment, skewness (γ), and forth moment, kurtosis (κ), of the delay distribution. Since the worst-case and best-case arriving timing (99.87% quantile, 0.14% quantile) are what designers mostly care about, estimating the full shape of the delay distribution is not most efficient. As a result, a cell delay calibration method is proposed in this section to coordinate the worst-case and best-case arriving time using skewness and kurtosis, Mathematically:

$$\begin{bmatrix} T(+3\sigma) \\ T(0\sigma) \\ T(-3\sigma) \end{bmatrix} = A * \begin{bmatrix} \mu \\ \sigma \\ \gamma\sigma \\ \kappa\sigma \\ \gamma\kappa\sigma \end{bmatrix} \quad (8)$$

$T(+3\sigma)$, $T(0\sigma)$ and $T(-3\sigma)$ representing the 99.87% quantile, 50% quantile and 0.14% quantile respectively. A is the calibration matrix between quantiles and moments computed using Matlab. Since skewness and kurtosis affecting the +/-3σ point simultaneously, a cross term $\gamma\kappa$ must also be considered. In MIS situation, the first and second moment can be substituted to μ_{ij} and σ_{ij} while the third and forth moment need no scaling since their influences are small.

IV. Results

A. SIS Cell Delay accuracy

The delay distributions of standard cells (NAND, NOR and AOI) are modelled and verified using TSMC 28nm PDK. The supply voltage is set to be 0.4V as sub-threshold region, 0.7V as near-threshold region, and 1.1V as normal threshold region. The accuracy of cell delay models are verified by comparing to the data obtained through SPICE simulations with 10k Monte Carlo samples under global and local variations. Table I shows the errors of estimated +/-3σ delay using LSN [2], LESN [3] and the proposed calibration method compared to SPICE simulation results. It reveals that our calibration method have competitive accuracy comparing to the LSN and LESN model, especially in sub-threshold voltage.

B. MIS Cell Delay accuracy

To validate the accuracy and efficiency of the proposed statistical MIS model, 1000 cases of cells (including NAND, NOR, AOI cells) with input arrival times in a close temporal proximity are extracted randomly. For each cases, multiple

Authorized licensed use limited to: Chinese University of Hong Kong. Downloaded on November 22,2026 at 12:59:36 UTC from IEEE Xplore. Restrictions apply.

TABLE I
ERRORS OF ESTIMATING +/-3σ DELAY USING LSN, LESN, AND PROPOSED CALIBRATION METHOD (FO4, 25°C)

Voltage	Cell Name	LSN [2]		LESN [3]		Ours	
		-3σ	+3σ	-3σ	+3σ	-3σ	+3σ
0.4V	NAND	5.32	6.07	2.46	1.67	**1.41**	**0.91**
	NOR	5.96	6.99	1.97	**1.82**	**1.79**	2.34
	AOI	6.32	7.82	**2.39**	3.62	2.43	**3.20**
0.7V	NAND	1.20	0.31	1.20	0.31	**0.24**	**0.11**
	NOR	0.41	**0.34**	**0.25**	0.74	1.54	0.37
	AOI	2.46	**1.02**	**1.34**	1.44	1.74	2.46
1.1V	NAND	1.23	0.98	1.26	1.17	**0.33**	**0.16**
	NOR	0.21	**0.18**	0.17	1.02	**0.16**	0.32
	AOI	1.40	1.71	**0.57**	**0.81**	1.12	0.84
Average Error		2.72	2.82	1.29	1.40	**1.20**	**1.19**

* Input transition time of the cell is constant (20ps)

** $Error = \frac{abs(sim-model)}{sim} * 100\%$

methods are implemented and compared as follows. Method I is similar to [5] and Method II is similar to [9]. SPICE Monte Carlo simulation is taken as golden results. Fig. 4 and Fig. 5 show the comparisons for the results of different methods in estimating the +/-3σ point values in a typical MIS situation under 0.7V and 0.4V, separately. The results at 1.1V are not given since the errors of both three methods are close between each other. It can be seen that our delay calibration method shows a relatively small error comparing to the golden results, in both the near-threshold voltage and the sub-threshold voltage.

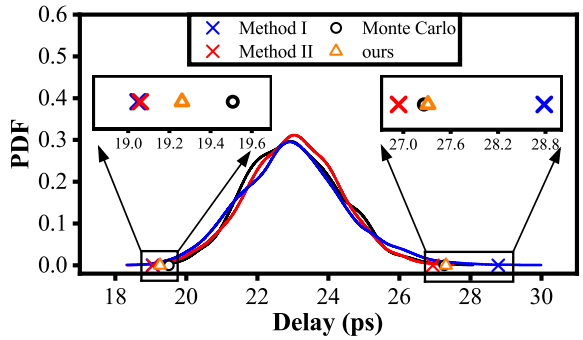

Fig. 4. Statistical MIS delay comparison for different methods of estimating the +/-3σ point (TSMC 28nm, 0.7V).

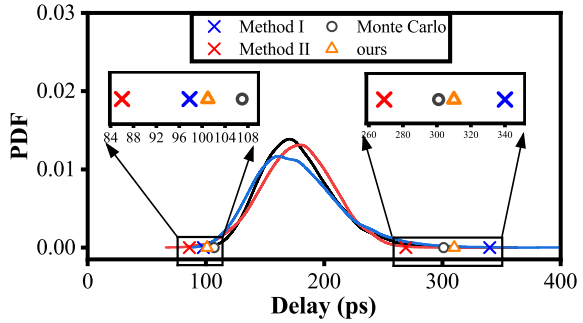

Fig. 5. Statistical MIS delay comparison for different methods of estimating the +/-3σ point (TSMC 28nm, 0.4V).

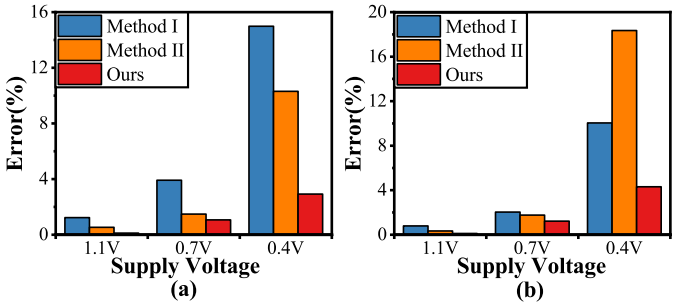

Fig. 6. (a) Errors of estimating -3σ point and (b) +3σ point comparison (Errors are calculated at 25°C through $Error = \frac{abs(sim-model)}{sim} * 100\%$).

Fig. 6 (a) and Fig. 6 (b) show the statistical MIS delay modelling accuracy comparison. It can be seen that as the voltage scales down, the Method I and II show a rising trend of error from under 2% to over 10% and from under 1% to over 15% respectively, while our proposed method is always under 5%. Moreover, our method shows a comparatively higher accuracy under different voltage, no matter estimating the -3σ point or the +3σ point. It should be noticing that as the voltage drops down, the Non-Gauss delay features become increasingly apparent, resulting in extra errors in calculation of (4) and (5). As a result, our method also shows a growth of error from less than 1% to around 4%, but it is within the acceptable range. On average, Method I and Method II show errors of 5.5% and 5.4% separately, while our method shows an error of 1.6%.

V. CONCLUSION

This paper presents a statistical cell delay model considering MIS effect. Based on TSMC 28nm technology library, the proposed method in MIS mode is more precise than prior MIS model and in SIS mode is competitively accurate with state-of-the-art SIS model.

ACKNOWLEDGEMENT

This work is supported by the National Nature Science Foundation of China (No. 62274034 and 61904030).

REFERENCES

[1] Kahng A B. 2015 52nd ACM/EDAC/IEEE Design Automation Conference (DAC). IEEE, 2015: 1-6.
[2] Balef H A, Kamal M, Afzali-Kusha A, et al. IEEE Transactions on Computer-Aided Design of Integrated Circuits and Systems, 2015, 35(9): 1503-1508.
[3] Jin L, Fu W, Yan H, et al. IEEE Transactions on Circuits and Systems II: Express Briefs, 2022, 69(6): 2932-2936.
[4] Shin J, Kim J, Jang N, et al. 2009 International SoC Design Conference (ISOCC). IEEE, 2009: 577-580.
[5] Fukuoka T, Tsuchiya A, Onodera H. IEICE transactions on fundamentals of electronics, communications and computer sciences, 2009, 92(12): 3070-3078.
[6] Tang Q, Zjajo A, Berkelaar M, et al. 2011 IEEE International Conference on IC Design & Technology. IEEE, 2011: 1-4.
[7] Sridharan J, Chen T. Proceedings of the Design Automation & Test in Europe Conference. IEEE, 2006, 1: 6 pp.
[8] Sinha D, Zhou H. ICCAD-2005. IEEE/ACM International Conference on Computer-Aided Design, 2005. IEEE, 2005: 837-843.
[9] Sinha D, Rao V, Peddawad C, et al. 2020 57th ACM/IEEE Design Automation Conference (DAC). IEEE, 2020: 1-6.

Authorized licensed use limited to: Chinese University of Hong Kong. Downloaded on November 22,2026 at 12:59:36 UTC from IEEE Xplore. Restrictions apply.